*Pure & Appl. Chem.*, Vol. 60, No. 10, pp. 1499–1516, 1988.
Printed in Great Britain.


# Molecular surface science of organic monolayers

G.A. Somorjai

Department of Chemistry and Center for Advanced Materials, Materials and Chemical Sciences, Lawrence Berkeley Laboratory, University of California, Berkeley, California 94720, U.S.A.

Abstract

The molecular structure of organic monolayers adsorbed on transition metal surfaces at low pressures can be studied by a combination of surface science techniques that include low energy electron diffraction (LEED) - surface crystallography, high resolution electron energy loss spectroscopy (HREELS) and scanning tunneling microscopy (STM). Most of the studies focussed on small alkenes and aromatic molecules that were adsorbed on flat, low Miller Index metal surfaces. The investigations were carried out in a wide temperature range and at various coverages. The results of these studies revealed that the surface chemical bonds of these molecules are very similar to those found in organo-metallic clusters. There is also temperature dependent rearrangements of the molecules leading to sequential bond breaking and to the formation of stable fragments at elevated temperatures. Adsorbate induced restructuring of the metal surfaces has also been observed.

Co-adsorption of two types of molecules can induce two-dimensional ordering if one of the adsorbates is a donor and the other is an acceptor. Co-adsorption can also modify the nature of bonding of the adsorbate to the metal by charge transfer through the metal.

The reaction intermediates during catalyzed hydrocarbon reactions are different from the stable organic adsorbates that bind strongly to the metal surface. Nevertheless, these tenaceous overlayers play significant roles in catalysis for hydrogen transfer and for providing sites for desorption. They also have significant roles in lubrication.

New surface science techniques can interrogate the solid-liquid and solid-solid interfaces as well. These include second harmonic and sum frequency generation that uses non-linear laser optics and the scanning tunneling and atomic force microscopes. Studies of organic monolayers using these techniques will also be discussed.

## INTRODUCTION

During the last ten years modern surface science techniques were applied to the study of the structure and bonding of monolayers of small organic molecules adsorbed on metal surfaces. In these investigations usually a 1 $cm^2$ area single crystal is used as a substrate.[1] Of the many tools of surface science, low energy electron diffraction (LEED) and high resolution electron energy loss spectroscopy (HREELS) produced most of the data, although infrared spectroscopy and synchrotron radiation methods have also contributed significantly. The studies revealed that 1) the surface chemical bonds of these molecules are very similar to those found in organo-metallic clusters. A unique feature is the temperature dependent variation of their bonding and sequential fragmentation that gives rise to the formation of organic moieties that are stable only in a well defined temperature range for a given metal surface.

The surface chemical bonds of organic molecules were also 2) dependent on the coverage and the coadsorption of two types of molecules, one donor and one acceptor, which can induce two dimensional ordering reflecting the importance of adsorbate-adsorbate interactions.

In this paper we shall briefly describe the experimental methodology used in these investigations of organic monolayers. Then we shall demonstrate the organo-metallic cluster nature and temperature dependence of the surface chemical bond and the importance of coadsorption. The possible role of the strongly adsorbed organic species in heterogeneous catalysis will be reviewed. Finally, we will discuss the emerging new techniques of research for the molecular level scrutiny of organic molecules at the solid-liquid and solid-solid interfaces.

### Experimental techniques to investigate structure and reactivity of organic monolayers

Low-energy electron diffraction[2] (LEED) and high-resolution electron energy loss spectroscopy[2] (HREELS) were the primary techniques used in our laboratory to study the structure and bonding of the organic monolayers. LEED has developed to the point where a complete set of diffraction beam intensities can be obtained in about 5 min over a 100-150-eV electron energy range by using computer-interfaced video camera

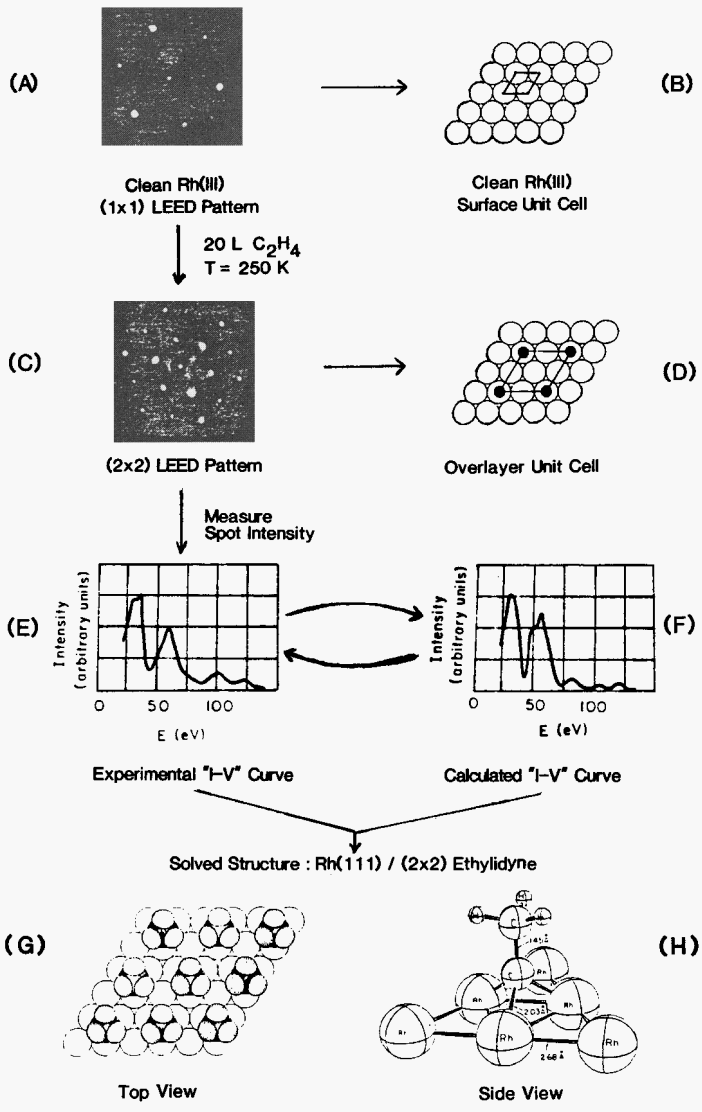


Figure 1 Outline of the steps involved in solving an adsorbate surface structure by low-energy electron diffraction (LEED) using the (2x2) structure of ethylidyne on Rh(111) as an example.

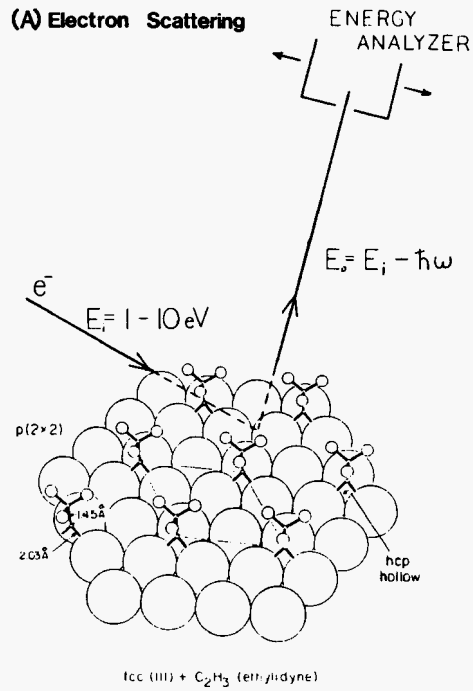


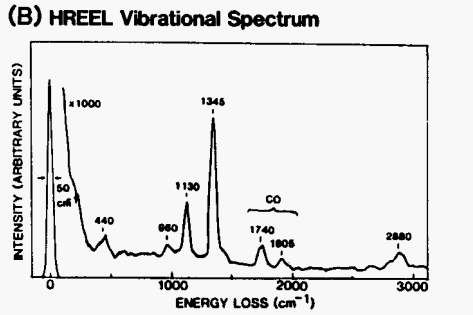


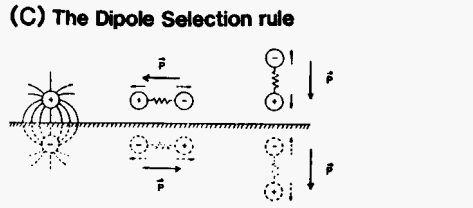


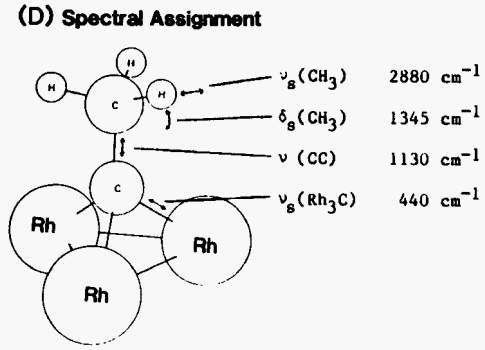


Figure 2 Principles of high-resolution electron energy loss spectroscopy (HREELS) as applied to a (2x2) monolayer of ethylidyne on Rh(111): (A) the experiment, (B) the spectrum, (C) the phenomena responsible for the dipole selection rule, and (D) the spectral assignment for ethylidyne.

instrumentation.[4] The recent development of digital LEED permits the use of nanoampere instead of microampere currents of the incident electron beam, so as to minimize or completely eliminate beam damage of the adsorbed species during the experiments. The theory of LEED has developed[5] rapidly over the past 10 years to permit the structure analysis of ordered layers of organic molecules of ever increasing size, including benzene and naphthalene. Recent theoretical advances permit the structure analysis of disordered adsorbed monolayers as long as the substrate is ordered.[6] The scheme of LEED-surface crystallography studies is shown in Figure 1.

HREELS determines the vibrational spectrum of adsorbed layers, ordered or disordered, with a typical energy resolution of 50 $cm^{-1}$. The technique permits us to independently obtain structural information[2] on the same adsorbate system that was studied with LEED. In addition, the vibrational spectra can be readily compared with spectra obtained from the organometallic molecules or multinuclear clusters. A wealth of infrared spectroscopy data exists in the literature on the vibrational spectra of these molecules, which permits us to compare their structure with those of the surface adsorbed species.[7] The scheme of HREELS-vibrational spectroscopy studies is presented in Figure 2.

Both LEED and HREELS studies have to be carried out at the low ambient pressures of ultra-high-vacuum ($10^{-9}$-$10^{-6}$ Torr). In order to investigate the behavior of organic monolayers when subjected to high-pressure gases or under catalytic reaction conditions at high pressures, a high-pressure/low- pressure reaction chamber is utilized.[8] The single-crystal sample (usually 1 $cm^2$ in size) can be isolated in a tube that is placed in the middle of the ultra-high-vacuum system containing the LEED or HREELS equipment. The tube can then be pressurized after closing and the catalytic reaction, such as ethylene hydrogenation, can be carried out at atmospheric pressures. The reaction rate and the product distribution can be monitored by a gas chromatograph. When the reaction is completed the reaction tube is evacuated and opened and the crystal surface is subjected to further studies by LEED, HREELS, or other surface techniques (Auger electron spectroscopy, for example). After surface analysis the crystal may be repeatedly exposed to high ambient pressures if desired.

## TALE OF TWO MOLECULES: STRUCTURES PRODUCED FOLLOWING ADSORPTION OF ETHYLENE AND BENZENE ON TRANSITION METAL SURFACES

### Surface structure of ethylene on transition metal surfaces

Figure 3 shows a temperature programmed desorption spectrum of the sequential dehydrogenation of adsorbed alkenes, ethylene, propylene and butene when adsorbed on a Pt(111) surface[9]. The molecules adsorb intact at the low temperatures. Upon heating, they loose hydrogen sequentially. Between the hydrogen desorption peaks there are

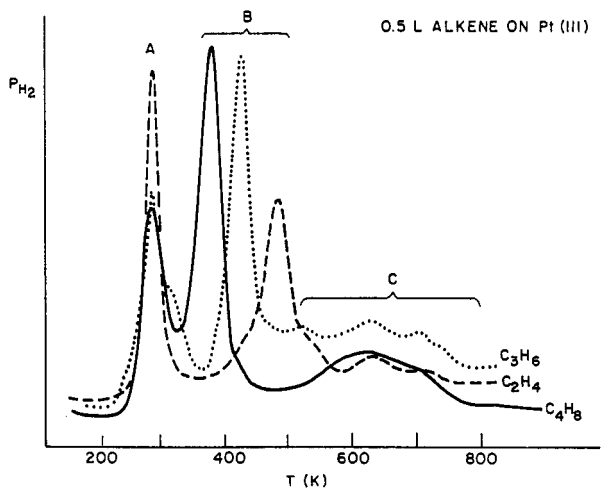


Figure 3 Hydrogen thermal desorption spectra from ethylene ($C_2H_4$), propylene ($C_3H_6$) and the 2-butenes ($C_4H_8$) adsorbed on Pt(111). Peaks A correspond to excess hydrogen desorbing directly from the metal. Peak B represent the first hydrogen atoms breaking off, while the peaks C originate from decomposition fragments.

temperature regimes where the stable partially dehydrogenated intermediates exist. It is of importance to understand the structure and bonding of these various organic adsorbates since only at the highest temperatures (800 K) do they dehydrogenate fully to leave behind a graphitic overlayer. Figure 4 shows the vibrational spectra obtained after ethylene desorption at 77K, 310K, and 450K[10]. The structure changes as the molecule becomes successively dehydrogenated. At low temperatures, ethylene is intact and its CC bond is parallel to the platinum surface. Such structures have their organo - metallic cluster compound equivalent as indicated by figure 5. As one

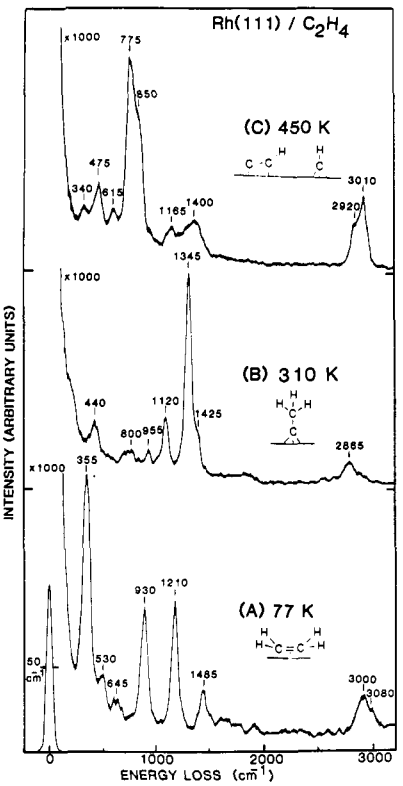


Figure 4

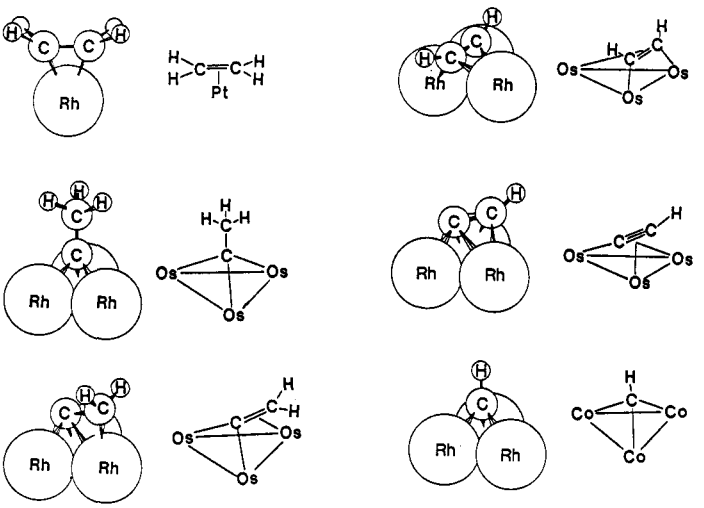

Figure 5

Figure 4 Specular HREEL vibrational spectra and proposed surface species for a saturation coverage of ethylene adsorbed on Rh(111) at: (A) 77 K, (B) 300 K and (C) 450 K. The spectra were taken at 77 K, 300 K and 300 K respectively.

Figure 5 Proposed surface species (left panel of each pair) compared with existing species in organometallic clusters (right panels).

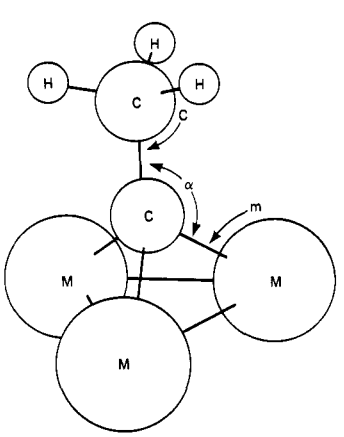

Different ethylidyne species: bond distances and angles
($r_C$ = carbon covalent radius; $r_M$ = bulk metal atomic radius)

| | C [Å] | m | $r_M$ | $r_C$ | $\alpha$ [°] |
|---|---|---|---|---|---|
| $Co_3(CO)_9CCH_3$ | 1.53 (3) | 1.90 (2) | 1.25 | 0.65 | 131.3 |
| $H_3Ru_3(CO)_9CCH_3$ | 1.51 (2) | 2.08 (1) | 1.34 | 0.74 | 128.1 |
| $H_3Os_3(CO)_9CCH_3$ | 1.51 (2) | 2.08 (1) | 1.35 | 0.73 | 128.1 |
| Pt (111) + (2 X 2) $CCH_3$ | 1.50 | 2.00 | 1.39 | 0.61 | 127.0 |
| Rh (111) + (2 X 2) $CCH_3$ | 1.45 (10) | 2.03 (7) | 1.34 | 0.69 | 130.2 |
| $H_3C-CH_3$ | 1.54 | | | 0.77 | 109.5 |
| $H_2C=CH_2$ | 1.33 | | | 0.68 | 122.3 |
| $HC\equiv CH$ | 1.20 | | | 0.60 | 180.0 |

Figure 6 Comparison of bond lengths and bond angles in surface- and cluster-bound ethylidyne species. Corresponding parameters for acetylene, ethylene and ethane are also given for comparison.

increases the temperature to 300 K, ethylidyne forms which is shown[11], separately in figure 6. To produce this molecule one hydrogen is eliminated. It has a stoichiometry $C_2H_3$ and a C-C bond that is perpendicular to the surface. On the (111) platinum or rhodium or other transition metal surfaces this molecule sits in a 3-fold site and its C-C bond is elongated to a single bond[12]. There are many organometallic multi-nuclear clusters exist with the same structure. These types of molecules are called alkylidynes thus, the name ethylidyne for ethylene absorbed with this type of bonding. In figure 7 there are several organometallic complexes shown with alkylidyne structures[10]. These are produced not only in 3-fold sites but they occur one, two and four coordinations as well. This type of bonding of adsorbed ethylene is prevalent around room temperature on most transition metal surfaces. They are also commonly occuring in multi-nuclear organometallic clusters.

Increasing the temperature converts the ethylidyne molecules to $C_2H$ and CH species. Figures 8 and 9 show several organometallic multi-nuclear complexes with these structures, again indicating that the adsorbed organic fragment on surfaces have structures identical to those in multi-nuclear organometallic clusters[13].

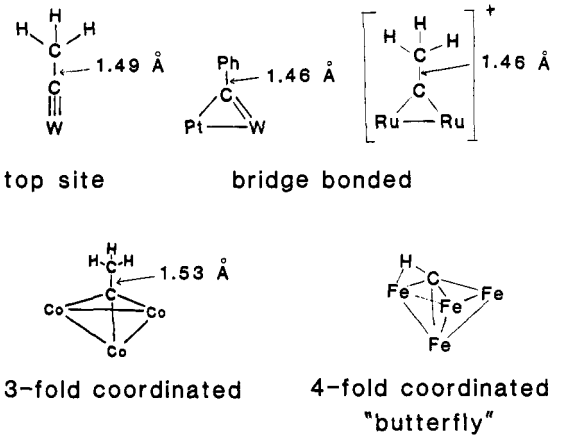


Figure 7

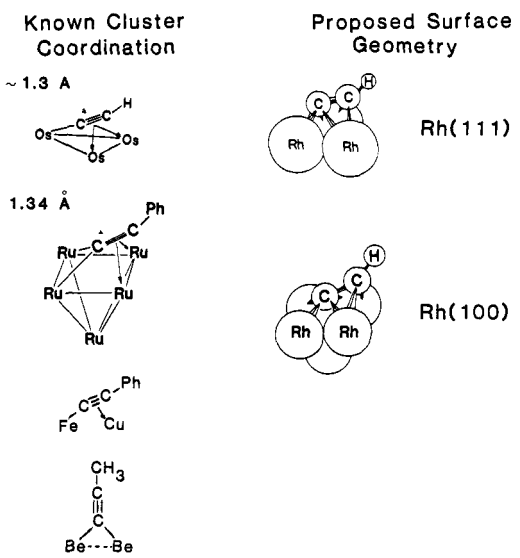


Figure 8

Figure 7 Comparison of the different types of alkylidyne coordination that are known for organometallic complexes.

Figure 8 Cluster bonding geometries known for the $C_2H$ ligand in organometallic chemistry along with the proposed $C_2H$ bonding geometries on Rh(111) and Rh(100).

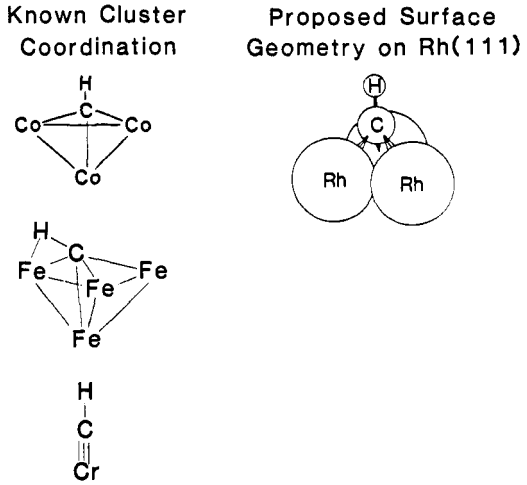


Figure 9
Cluster bonding geometries known for the CH ligand in organometallic chemistry along with the proposed CH bonding geometry on Rh(111).

**Probable reaction paths for the surface rearrangements of adsorbed ethylene**

Recent theoretical calculations[14] suggest smaller activation energies for the conversion of adsorbed molecular ethylene to ethylidyne if the molecule is hydrogenated first to $C_2H_5$ and then dehydrogenated to $C_2H_3$ rather than losing a hydrogen atom directly. These two possible reaction pathways are shown in Figure 10a. In the hydrogenation/dehydrogenation mechanism, the source of the adsorbed hydrogen needed for the initiating hydrogenation step is either the ambient of the ultra-high-vacuum chamber that always contains residual amounts of $H_2$ or the lower temperature dehydrogenation of an ethylene at a surface imperfection. Each successive conversion of ethylene to ethylidyne then produces an additional surface hydrogen atom. Figure 10b shows the calculated activation energies for the formation of $C_2H$ species from the ethylidyne. The experimental results[10,11] correlate well with these computational findings.

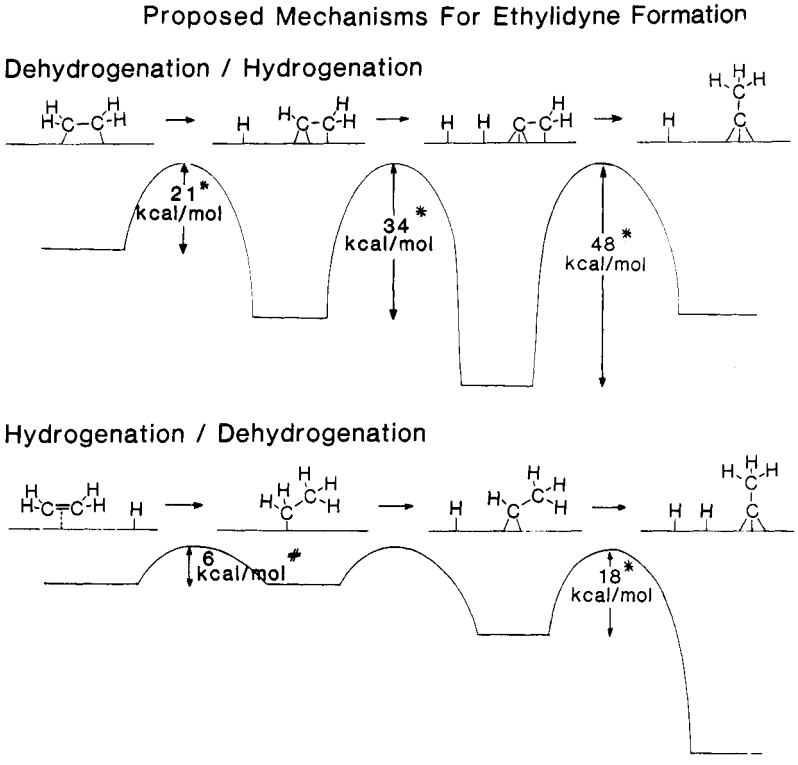


Figure 10a Schematic representation of the surface intermediates and energetics for the previously postulated dehydrogenation/ hydrogenation mechanism and the newly proposed hydrogenation/dehydrogenation mechanism for ethylidyne formation on transition-metal surfaces.

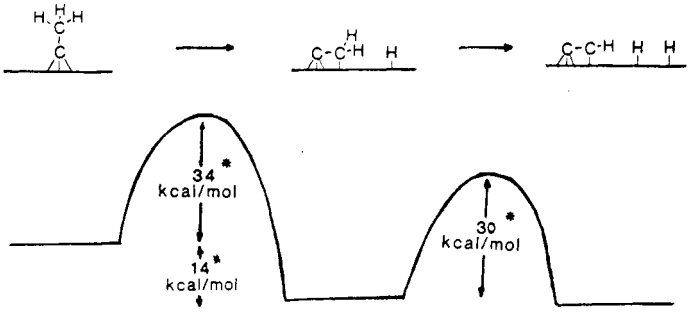


Figure 10b A proposed mechanism for conversion of ethylidyne ($CCH_3$) to vinylidene ($CCH_2$) and acetylide (CCH). Energetics shown were calculated by molecular orbital methods for a Pt(111) slab.[14]

## Structure and bonding of benzene on transition metal surfaces

Figure 11 shows the vibrational spectra of benzene and several transition metal surfaces. These types of spectra along with low energy electron diffraction determinations of its surface structures indentify the structures of benzene on various transition metal surfaces that are shown in Figure 12. Ordering of the adsorbed benzene molecules requires co-adsorption[15] with carbon monoxide that will be discussed in detail later. On Pd(111) benzene has a gas phase-like structure with its $\pi$-ring parallel to the metal surface[16,17,18,19]. The center of the molecule is in a 3-fold hollow and the bond distances are very similar to those of gas phase benzene. This is not the case on the Pt(111) surface which is also shown in the figure. Benzene is situated in a bridge site, on this surface the $\pi$-ring is parallel to the surface but the C-C distances are greatly distorted. Four C-C bonds are longer than the other two. Figure 12 shows another benzene structure on the Rh(111) surface, in this case the molecule is in a 3-fold hollow site and the CC-bonds are alternating between a very long 1.81Å and a short 1.33Å as determined by LEED surface crystallography. This molecule behaves almost as there were three acetylene molecules bound together. However, vibrational spectroscopy clearly indicate that the breathing modes of the $\pi$-ring are detectable for this highly distorted benzene molecule. Figure 13 shows a ruthenium tri-nuclear cluster

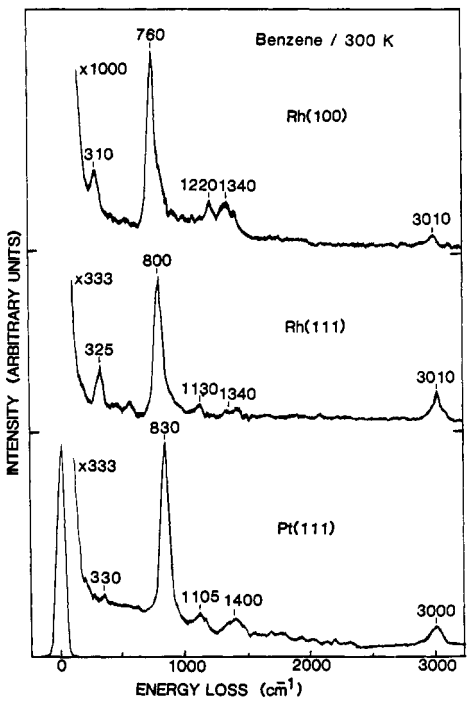


Figure 11
HREEL vibrational spectra for benzene adsorbed on Rh(100), Rh(111) and Pt(111) at room temperature

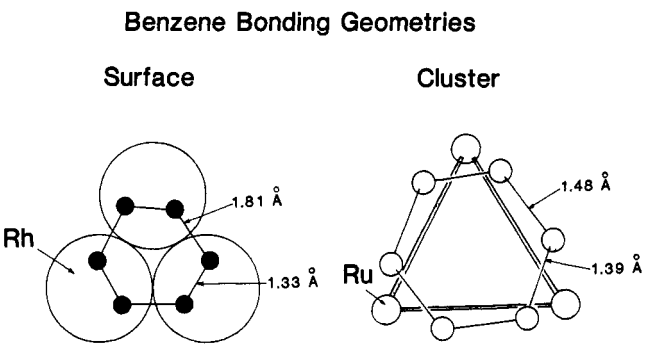


Figure 13 Comparison of the adsorption structure of benzene on the Rh(111) surface with the structure of benzene attached to $Ru_3$ cluster.

| Substrate | (Gas Phase) | Pd(111) | Rh(111) | | Pt(111) |
|---|---|---|---|---|---|
| Surface Structure | | (3x3)-$C_6H_6$ + 2CO | (3x3)-$C_6H_6$ + 2CO | c(2$\sqrt{3}$x4)rect-$C_6H_6$ + CO | (2$\sqrt{3}$x4)rect-2$C_6H_5$ +4CO |
| The Structure of Benzene | 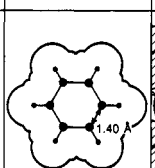 | 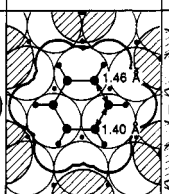 | 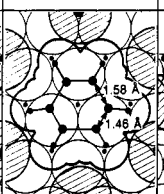 | 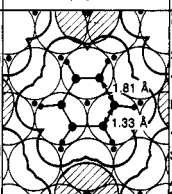 | 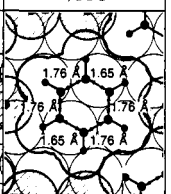 |
| $C_6$ Ring Radius (Å) | 1.40 | 1.43±0.10 | 1.51±0.15 | 1.65±0.15 | 1.72±0.15 |
| $d_{M-C}$(Å) | - | 2.39±0.05 | 2.30±0.05 | 2.35±0.05 | 2.25±0.05 |
| $\gamma_{CH}$(cm$^{-1}$) | 670 | 720-770 | 780-810 | | 830-850 |

Figure 12 Comparison of the adsorption structure of benzene on Pd(111), Rh(111) and Pt(111) with gas-phase benzene. The benzene is coadsorbed with CO on the three metal surfaces, with two relative concentrations on Rh(111). Tabulated are the average $C_6$ ring radius, the metal-carbon distance and the vibrational frequency of the benzene "umbrella" mode.

of benzene that is also distorted indicating that the organometallic cluster nature of the surface species also holds for the aromatic molecules[20].

Figure 14 shows that ethylene and benzene while having difference structures at low temperatures, above 400K form identical surface species which are acetylide, $C_2H$, and methylidyne, CH. Thus, while at low temperatures the adsorbed organic molecules may have different structures and bonding, above a certain temperature they all form the same fragments. A proposed reaction path for the decomposition of benzene on metal surfaces is shown in Figure 15. Three acetylene molecules form which cannot be detected but should be a likely intermediates which then dehydrogenate to form the $C_2H$ acetylide species[21]. $C_2H$ and CH are detectable on all transition metal surfaces upon heating adsorbed benzene to elevated temperatures[22].

The bonding of aromatic molecules other than benzene are more complicated indicated by recent studies of pyridine on transition metal surfaces[23]. This molecule is tilted at a 45 degree angle with respect to the surface plane on the Rh(111) surface and depending on coverage or on the nature of the transition metal or its structure it may lie flat on the surface or at an angle or perpendicular to the surface bonding through the lone pair of electrons of the nitrogen in the aromatic ring. Figure 16 shows different bonding arrangements of pyridine as detected by surface science on various transition metal surfaces using LEED and HREELs.

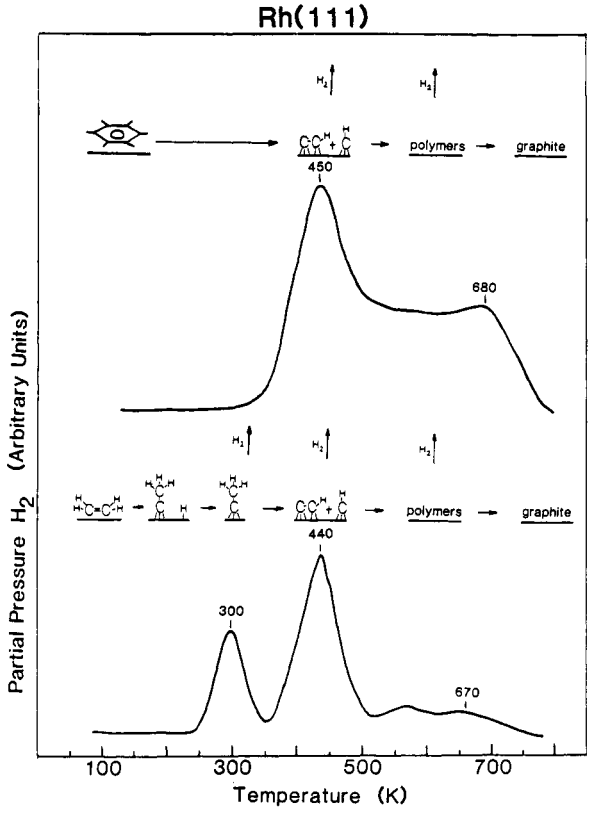


Figure 14
Hydrogen thermal desorption from benzene (top curve) and ethylene (bottom curve) adsorbed on Rh(111), with indication of fragmentation pathways.

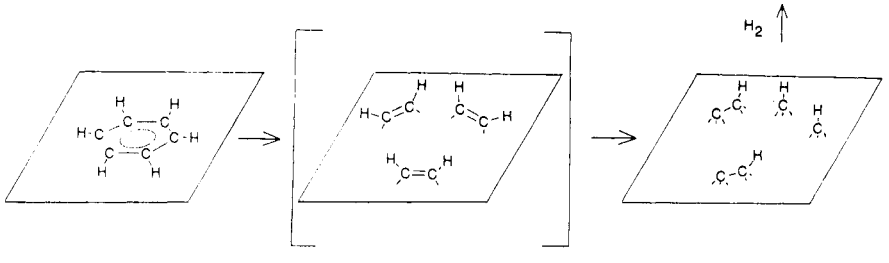


Figure 15 Proposed pathway for benzene decomposition on Rh(111).

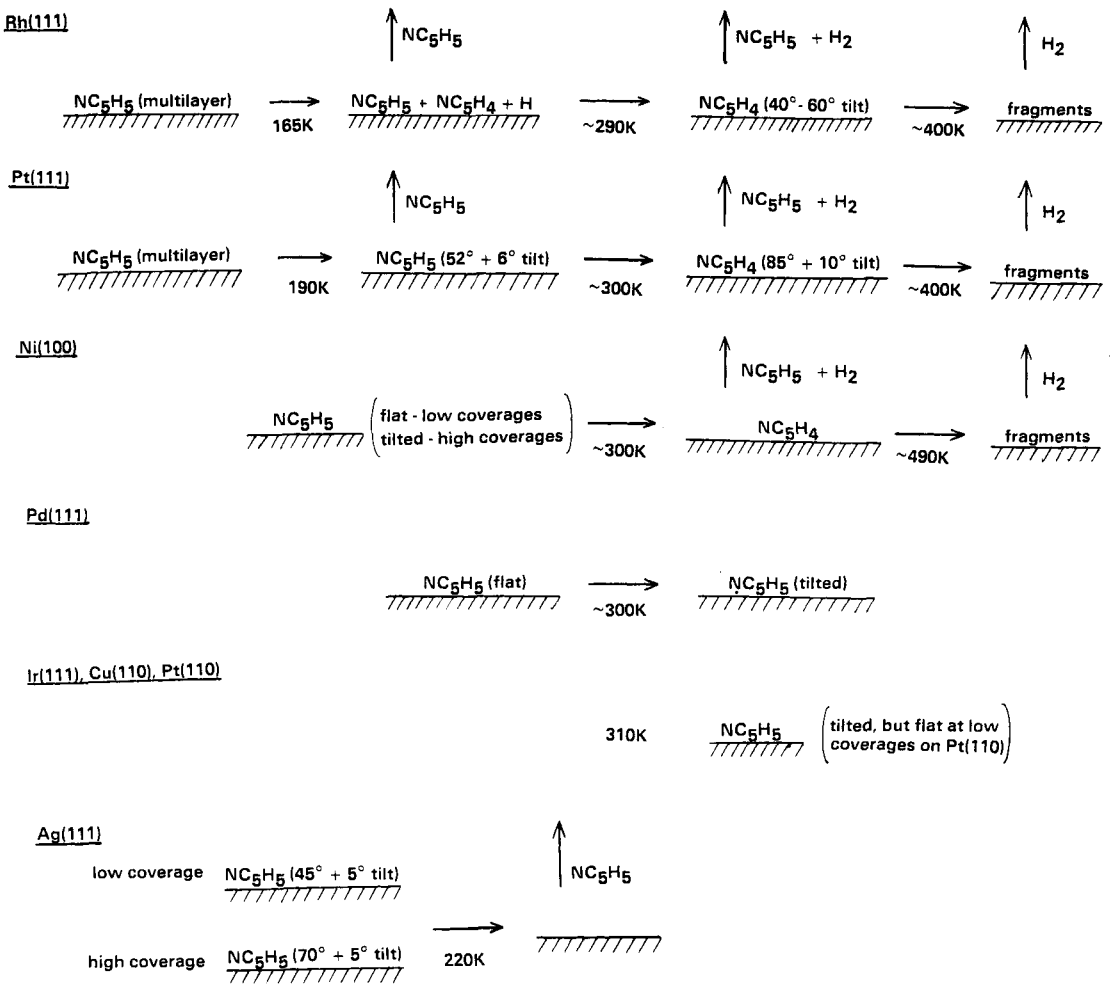


Figure 16 Structural rearrangements and thermal decomposition of pyridine, $NC_5H_5$ following adsorption on various transition metal surfaces.

## Are strongly adsorbed organic species on transition metal surfaces intermediates for catalytic reactions?

Ethylene readily hydrogenates to ethane in the presence of excess hydrogen on most transition metal surfaces. Low energy electron diffraction and high resolution electron energy loss spectroscopy studies were carried out on single crystal surfaces that were utilized for ethylene hydrogenation, and these studies revealed the presence of a monolayer of ordered ethylidyne molecules when both Rh(111) and Pt(111) crystal surfaces are very active for the hydrogenation reaction. $^{14}C$ labeling of the carbon on the adsorbed ethylidyne monolayer during the hydrogenation reaction is about a million times greater than the rate of ethylidyne removal. Adsorbed $C_2H_3$ is a spectator rather than a reactant on the metal surfaces.

There is evidence from other studies of the hydrogenolysis of ethane to methane on transition metal surfaces that ethylidyne can indeed be one of the intermediates for the reaction. The role of the strongly adsorbed monolayer of organic species on surfaces during catalytic reaction is complex. It should be examined for each catalytic reaction in question. It is likely the higher the temperature of the reaction and the higher the activiation energy for the reaction, the more likely that the strongly adsorbed surface species may be reaction intermediates. For more facile reactions, it is unlikely that the strongly adsorbed organic species in the surface monolayer plays a significant role during the reaction.

## COADSORPTION

Carbon monoxide induces order in adsorbed benzene overlayers on Rh(111) and Pt(111) surfaces has been reported recently[15]. Since that initial report, carbon monoxide induced ordering has also been observed for a wide variety of adsorbates {acetylene [24,25,26], ethylidyne ($\equiv CCH_3$) [24,26,27,28], propylidyne ($\equiv CHCH_2CH_3$) [24,26,29], benzene [26,28,30,31,32,33], fluorobenzene [24,26], sodium [24,26], potassium [34,25], and hydrogen [36]} on several metal surfaces {Rh(111) [24-25,29-31], Pt(111) [15,31,32], Pd(111) [33], Rh(100) [28], Ru(001) [34], Ni(100) [36], and Ni(110) [35]}. In these cases, the coadsorption of CO with another adsorbate results in the formation of new ordered surface structures different from those formed when either CO or the other adsorbate are present alone on these surfaces. The formation of these ordered, coadsorbed structures provides an excellent opportunity for studying the interaction between coadsorbed atoms and molecules under conditions where the relative geometry and stoichiometry can be established.

In this paper we show that the CO induced ordering with several coadsorbates - sodium, benzene, fluorobenzene, and ethylidyne - on the Rh(111) crystal surface and the reduction in the C-O stretching frequency can be correlated with the surface dipole moments of the adsorbates. Here, the surface dipole moments are determined by measuring work function changes as a function of adsorbate coverages. We find that CO induced

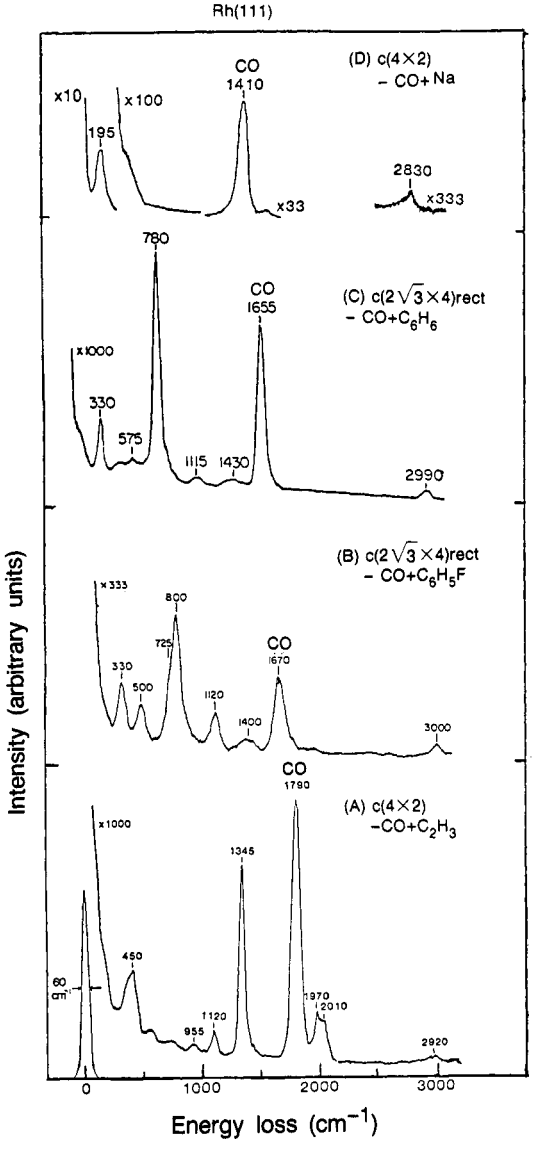


Figure 17
Vibrational spectra obtained by HREELS for the ordered, coadsorbed structures on Rh(111) at 310 K where there is one CO molecule per coadsorbate.

TABLE 1. CO-induced ordered structures on the Rh(111) surface.

| Coadsorbate | LEED Structure* | No. of Rh surface atoms per unit cell | No. of coadsorbates per unit cell | No. of CO's per unit cell | C-O stretching frequency(ies) ($cm^{-1}$) |
|---|---|---|---|---|---|
| -- | (√3x√3)R30° | 3 | 0 | 1 | 2010 (top) |
| -- | (2x2) | 4 | 0 | 3 | 2060 (top)<br>1855 (bridge) |
| ethylidyne ($\equiv CCH_3$) | c(4x2) | 4 | 1 | 1 | 1790 (hcp hollow)# |
| propylidyne ($\equiv CCH_2CH_3$) | (2√3x2√3)R30° | 12 | 3 | 1 | 1750 |
| Acetylene ($C_2H_2$) | c(4x2) | 4 | 1 | 1 | 1725 |
| Fluorobenzene ($C_6H_5F$) | (3x3) | 9 | 1 | 2 | 1720 |
| | c(2√3x4)rect | 8 | 1 | 1 | 1670 |
| Benzene ($C_6H_6$) | (3x3) | 9 | 1 | 2 | 1700 (hcp hollow)# |
| | c(2√3x4)rect | 8 | 1 | 1 | 1655 (hcp hollow)# |
| Na | (√3x7)rect | 14 | 4 | 7 | 1695 |
| | c(4x2) | 4 | 1 | 1 | 1410 |

*The notation (mxm) indicates a hexagonal unit cell with sides m times as long as the (1x1) unit cell sides; R30° means the unit cell is rotated 30° with respect to the (1x1) unit cell. The notation (m√3xn)rect indicates a rectangular unit cell with sides m√3 and n times as long as the (1x1) cell sides; the prefix "c" means the unit cell is a "centered" unit cell rather than a "primitive" unit cell.

#hcp hollow means one second layer metal atom lies below the three-fold hollow site, in contrast to a fcc hollow where no second layer atom lies below the three-fold site.

ordering occurs when CO is coadsorbed with an adsorbate that has a surface dipole moment oriented opposite to that of adsorbed CO, while disorder or segregation occurs when CO is coadsorbed with an adsorbate that has a similarly oriented dipole moment. We also find that NO, a ligand chemically similar to CO has a surface dipole moment opposite that of ethylidyne when coadsorbed in the c(4x2) - NO + ethylidyne structure. Further, the magnitude of the reduction in the C-O stretching frequency appears to be directly related to the surface dipole moment of the coadsorbate.

Our laboratory has already reported several studies [24-27,29-31] for the individual CO coadsorption systems on the Rh(111) surface. For the various ordered structures observed, Table 1 lists the LEED structures, the unit scell size, the types and number of adsorbates per unit cell, and the C-O stretching frequency(ies) of the adsorbed CO molecules. Most of our information concerning the adsorbates within the ordered, coadsorbed structures has come form vibrational spectra obtained by high-resolution electron energy loss spectroscopy (HREELS). Figure 17 shows the vibrational spectra for four of the ordered structures where there is one CO molecule per coadsorbate. The vibrational spectra show that both CO and the coadsorbate maintain their molecular identity within the ordered, coadsorbed structures and are discussed in detail elsewhere [15,24,26,27].

For several of the CO coadsorbed structures [27,30], Van Hove and co-workers have determined by dynamical LEED analyses the adsorption geometries of the coadsorbed molecules including the bond lengths and bond angles. Table 1 also indicates the CO adsorption sites within the ordered structures, as determined by the LEED analyses. In all the CO coadsorbed structures on Rh(111) solved by LEED, the adsorption site of CO is an hcp hollow site, where one second layer rhodium atom sits below the three-fold site occupied by the CO molecule.

From Table 1 and Fig. 17 we see that C-O stretching frequency is greatly reduced from that of CO adsorbed alone on Rh(111) on either top or bridge sites and ranges from 1790 $cm^{-1}$ for CO in the c(4x2)-CO + $CCH_3$ structure to 1410 $cm^{-1}$ in the c(4x2)-CO + Na structure. If we assume that CO bonds at hollow sites in all of the coadsorbed structures, as borne out for those structures that have been determined by dynamical LEED analysis, then the 380 $cm^{-1}$ spread of C-O stretching frequencies would indicate that interactions of varying strength occur between the CO molecule and the different coadsorbates.

Reduction in the C-O stretching frequency can arise from a combination of several interactions: (1) a vibrational Stark effect from the electric field generated by neighboring dipoles, (2) charge transfer through the substrate into the $2\pi^*$ orbital of coadsorbed CO, and (3) direct chemical interactions between the coadsorbates. As the work function measurements show, the coadsorbed molecules order when oppositely oriented dipoles are present in the unit cell. Thus, dipole-dipole interactions probably play a major role in the formation of coadsorbed structures. By using model calculations, it can be shown that the dipole-dipole interaction energy between coadsorbate pairs ranges from -0.09 eV for the c(2√3x4)rect CO + $C_6D_6$ structure to -0.7 eV for the c(2x4) Na + CO structure on Rh(111).

Figure 18 shows the work function change as a function of CO coverage on Rh(111). The coverage is defined as the ratio of adsorbed molecules per rhodium surface atoms. CO coverages were determined from the CO thermal desorption yield and calibrated against the LEED $(\sqrt{3}x\sqrt{3})R30^{\circ}$ structure, which forms at 0.33 of a monolayer. For CO coverages less than 0.33, where CO bonds only on top of the rhodium surface atoms, the work function change may be fit with a classical model for mobile adsorption. If we consider a well separated adsorbed species with surface density N, an initial dipole moment $\mu$, and polarizability $\alpha$, then the work function change ($\Delta\phi$) is given (in SI units) by

$$\Delta\phi = \frac{-eN\mu}{\varepsilon_0[1 + (9/4\pi)\alpha N^{3/2}]}$$

where $\varepsilon_0$ is the vacuum permittivity. A good fit for $\theta_{CO} \leq 0.33$ can be obtained with $\mu_{CO} = 0.67 \times 10^{-30}$ C•m (~0.2D) and $\alpha_{CO} = 0.34 \times 10^{-28}$ $m^3$.

For $\theta_{CO} > 0.33$, $\Delta\phi$ increases dramatically until reaching a value of +1.05 eV at saturation coverage ($\theta_{CO} = 0.75$), where a (2x2) LEED pattern was observed. To achieve the (2x2) LEED structure, we found it necessary to cool the sample to 170 K, while the

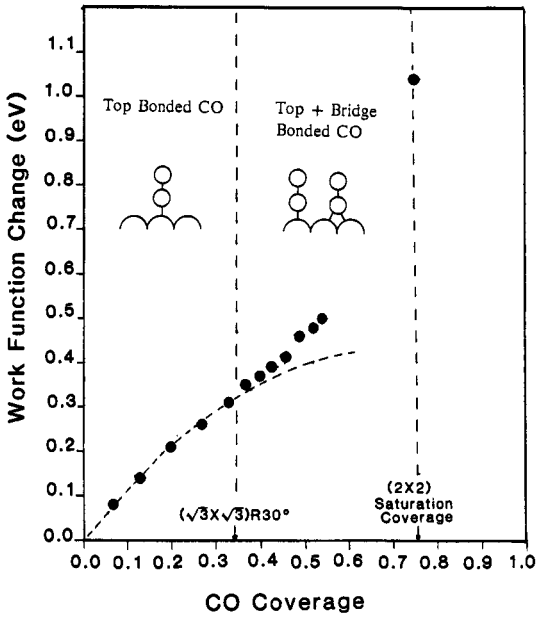


Figure 18
The work function change of the Rh(111) surface as a function of CO coverage. The dashed curve shows the fit with the model discussed in the text.

TABLE 2
Combinations of adsorbates with similarly oriented dipole coadsorbed on the Rh(111) surface.

| Coadsorbates | LEED Patterns Observed |
|---|---|
| CO + NO | Disordered or compressed (2x2)-3CO [26] |
| Na + $C_2H_2$ | Disordered |
| Na + $\equiv CCH_3$ | Disordered |
| Na + $C_6H_6$ | $(\sqrt{3}x\sqrt{3})R30^\circ$ + $(2\sqrt{3}x3)$rect* |

*Since the $(\sqrt{3}x\sqrt{3})R30^\circ$ and $(2\sqrt{3}x3)$rect are observed for Na and benzene, respectively, adsorbed alone on Rh(111), the observation of a mixture of these two LEED structures implies that these two coadsorbates segregate on the surface.

other CO coverages could be obtained at room temperature. For $\theta_{CO} > 0.33$, some of the adsorbed CO bonds bridging two rhodium atoms as well as on top sites [38,40]. We attribute the dramatic increase in $\Delta\phi$ for $\theta_{CO} > 0.33$ to bridge bonded CO molecules on Rh(111) having a larger surface dipole moment than top bonded CO. Since we are unable to determine the relative coverages of bridge and top bonded CO between 0.33 and 0.75 monolayer coverages, we are unable to model this system in order to determine the surface dipole moment or polarizability for bridge bonded CO on this surface.

Adsorbed CO has a negative surface dipole moment, while the other adsorbates, which all form ordered structures with coadsorbed CO, have positive surface dipole moments, opposite that of adsorbed CO. Therefore, it appears that CO-induced ordering occurs when CO is coadsorbed with an adsorbate with an oppositely oriented surface dipole moment.

To further test the hypothesis that ordering of coadsorbed molecules is driven by having oppositely oriented dipole moments within the ordered unit cells, we have coadsorbed molecules whose surface dipole moments are nominally oriented in the same direction and have found these combinations are disordered or segregated. Table 2 lists these results. In these experiments we tried to coadsorb the molecules at coverages and conditions similar to those where CO induced ordering of coadsorbed structures were observed. It appears that the dipole-dipole interaction energy promotes the formation of the coadsorbed structures for oppositely oriented dipoles but not for similarly oriented dipoles.

We have also measured the work function for several of the ordered structures formed with coadsorbed CO on Rh(111). Table 3 lists the work functions observed for the structures formed by the organic adsorbates, both with and without coadsorbed CO. As can be seen from Table 3, the work function increases as the ratio of CO's to coadsorbates is increased, indicating that CO still has a negative surface dipole moment within the coadsorbed structures. Accurate determination of the dipole moments within the coadsorbed structures is difficult and would require detail measurements of work function changes as a function of coverage of both surface species. However, if we assume that benzene, fluorobenzene, and ethylidyne have the same surface dipole moment when coadsorbed with CO as when adsorbed alone on Rh(111), then we are able to estimate that CO has an effective surface dipole moment of $\sim -2.4 \times 10^{-30}$ C•m (-0.8 D) in the structures listed in Table 4. The assumption that benzene, fluorobenzene, and ethylidyne have the same dipole moments when coadsorbed with CO as when adsorbed alone is reasonable since previous HREELS [15,24,26,27] studies indicate no significant changes in the adsorbate's internal structure when coadsorbed with CO.

TABLE 3

Work function of the Rh(111) surface at 310 K for various ordered structures, with and without coadsorbed CO. The work function of a bare Rh(111) surface is 5.4 eV [22].

| Coadsorbate | | Number of CO's per Coadsorbate | | |
|---|---|---|---|---|
| | | 0 | 1 | 2 |
| $C_6D_6$* | LEED Structure | (2√3x3)rect | c(2√3x4)rect | (3x3) |
| | Work Function (eV) | 4.04 | 4.76 | 5.14 |
| $C_6D_5F$* | LEED Structure | (√19x√19)R23.4° | c(2√3x4) rect | (3x3) |
| | Work Function (eV) | 4.16 | 4.79 | 5.16 |
| $\equiv CCH_3$ | LEED Structure | disorder | c(4x2) | -- |
| | Work Function (eV) | 4.17 | 5.08 | -- |

*The deuterated molecule was used in order to avoid interference from the background hydrogen in TDS measurements.

TABLE 4

Calculated electric fields and interaction energies for ordered arrays of dipoles.

| Structure | Electric field (V/Å) at the CO | at the coadsorbate | Interaction energy (eV) |
|---|---|---|---|
| c(4x2)-CO+$CCH_3$ | -0.23 | 0.098 | -0.1 |
| c(2√3x4)rect-CO+$C_6D_6$ | -0.23 | -0.46 | -0.09 |
| c(4x2)-CO+Na | -1.5 | -0.56 | -0.7 |

We have also measured the work function change when NO, a ligand chemically similar to CO, is coadsorbed with a saturation coverage of ethylidyne. NO, like CO, forms a c(4x2) LEED structure on Rh(111) when coadsorbed with ethylidyne, but the ethylidyne species bonds at an hcp hollow site when coadsorbed with NO rather than at the fcp hollow site it bonds at when adsorbed alone or with CO [5]. When NO is coadsorbed to form the c(4x2) structure, the work function increases by 0.45 eV, indicating that NO, like CO, has a negative dipole moment when coadsorbed with ethylidyne.

A necessary condition for the formation of intermixed, ordered structures when CO is coadsorbed with other adsorbates is that the Helmholtz free energy is less for the ordered structure compared to that of a disordered overlayer:

$$F_{ordered} - F_{disordered} = (U_{ordered} - U_{disordered}) - T(S_{ordered} - S_{disordered}) < 0$$

The difference in free energy, $\Delta F = F_{ordered} - F_{disordered}$, between an ordered and disordered overlayer is composed of two terms -- an entropy term, $T\Delta S = T(S_{ordered} - S_{disordered})$ that drives the system toward disorder and an interaction energy term, $\Delta U = U_{ordered} - U_{disordered}$ that drives the system toward order.

Our results indicate that the interaction energy, ΔU, favors ordered, coadsorbed systems when the coadsorbed molecules have oppositely oriented surface dipoles.

Obviously, oppositely oriented dipoles are attracted to each other, while similarly oriented dipoles repel each other. To have a better feel for the magnitude of the dipole-dipole interaction energies of coadsorbed molecules, we have carried out model calculations for ordered arrays of dipoles to compute the dipole-dipole interaction energies for several of the ordered, coadsorbed structures on Rh(111), as well as the dipole electric fields normal to the surface within the unit cells. For these model calculations we make the simplifying approximation that the dipole moments of the coadsorbed species can be treated as point dipoles in the same plane. We also assume that CO has a dipole moment of $-2.4 \times 10^{-30}$ C•m, the estimated value for coadsorbed CO, while the other coadsorbates are assumed to have the dipole moments measured when adsorbed alone on Rh(111). The results of these calculations are listed in Table 4. The interaction energies in Table 4 are defined to be the difference, per CO-coadsorbate pair, between the dipole-dipole interaction energy of the dipoles in a coadsorbed lattice and the case where the dipoles are in two separate lattices. The negative sign for the interaction energy indicates that the coadsorbed structures are more energetically favorable, as one would expect for oppositely oriented dipoles. The dipole-dipole interaction energies range from -0.09 eV for the c(2√3x4)rect-CO + benzene structure to -0.7 eV for the c(4x2)-CO + Na structure. The CO + Na dipole-dipole interaction energy of 0.7 eV is comparable to the CO-Rh surface bond energy of 1.4 eV obtained from a thermal desorption measurement [41].

Norskov et al., [42] have theoretically investigated in more detail the dipole-dipole interaction of two coadsorbed species using effective medium theory to consider the effect the electrostatic potential induced by one adsorbate has on a neighboring adsorbate. These calculations take into account the rearrangement of charge between the adsorbates and the surface as well as the effect of screening of the electrostatic potential by the metal. They find, for example, that the interaction energy for CO and potassium coadsorbed on Fe(110) is in the range between 0.1 to 0.3 eV, smaller than the value of 0.7 eV that we estimate for Na and CO on Rh(111), probably because our calculations do not include screening effects.

It is reasonable to ask if any direct interactions (not through the substrate) occur between the coadsorbates other than dipole-dipole interactions. Other types of direct interactions for most of the coadsorbed structures are unlikely except maybe for Van der Waals interactions, as the coadsorbed molecules are found to be separated by at least their Van der Waals dimensions in those cases where the structure has been determined by a dynamical LEED analysis [27,30]. The Van der Waals interactions between closely packed adsorbed molecules, however, can be quite significant as shown by Gavezzotti et al., [43]. For example, these authors have calculated a Van der Waals packing energy of -0.12 eV per molecule (-2.7 kcal/mole) for benzene in a c(2√3x4) rect unit cell without coadsorbed CO, the same order as dipole-dipole interaction energies. A case where a strong, direct interaction may occur is for CO coadsorbed with Na in the c(4x2) structure. The very low C-O stretching frequency of 1410 $cm^{-1}$ is less than the value of 1445 $cm^{-1}$ observed of CO in the CO-alkali complex of potassium deltate, $K_2(CO)_3$ [41] suggesting that CO and Na may form a chemical complex on the surface [44].

Next we comment on interactions occurring through the metal substrate. For CO adsorbed alone on Rh(111), Ruckenstein and Halachev[45] have calculated the energies of interactions mediated by the substrate for various separation distances. They find interaction energies of a few hundredths of an eV that are positive (repulsive) for small separation distances and negative (attractive) for intermediate distances. Within the coadsorbed, ordered structures, the CO molecules are separated by intermediate distances (4 to 8 Å), so the CO-CO interactions should be attractive, which will further help to stabilize the ordered structures.

Another possible interaction, mediated by the metal surface, is charge transfer from one adsorbate to another through the substrate. Such an interaction has been widely discussed in the literature to occur between CO and alkali adatoms coadsorbed on metal surfaces [34,46,47,48]. Here, the electropositive alkali adatom is thought to donate charge to the surface, which is then backdonated into the $2\pi^*$ orbital of adsorbed CO. It is tempting to suggest that the surface dipole moments measured in our experiments are related to the amount of charge transfer between the adsorbates and the surface. While this may be the case for an alkali atom, like sodium, adsorbed on a metal surface [36], the situation for the molecular adsorbates is more complex, since they can also have a dipole moment associated with their molecular structure, as well as one associated with charge transfer to the surface. However, the vibrational frequencies of coadsorbed CO indicate that some degree of charge transfer into the $2\pi^*$ orbital of CO occurs for several of the coadsorbed structures.

Finally, we should mention that the addition of CO to an adsorbed overlayer can also reduce the entropy of the system. The reduction in entropy comes about from CO blocking not only its own adsorption site, but, due to steric effects, also prevents coadsorbates from occupying neighboring sites. For example, CO when coadsorbed with benzene blocks a total of seven hcp hollow sites from benzene adsorption on Rh(111). Since the sites blocked by an adsorbed CO become correlated with each other, the number of possible configurations for the coadsorbed system is reduced along with the entropy of a disordered overlayer, thereby making an ordered overlayer relatively more energetically favorable. Also, as the entropy for an intermixed overlayer is higher than for a segregated overlayer, the entropy helps promote intermixed structures over segregated structures. Even though entropy considerations help to explain why ordered, coadsorbed structures occur they do not account for only coadsorbed structures with oppositely oriented dipoles being observed, indicating that interaction energies play a dominant role.

The correlation between the C-O stretching frequency and the surface dipole moment of the coadsorbates can be seen most effectively by plotting the C-O stretching frequency vs. the dipole moment, as shown in Fig. 19, for the coadsorbed, ordered structures where there is only one CO per coadsorbate. Even though only a few data points are available, it appears that the larger the surface dipole moment of the

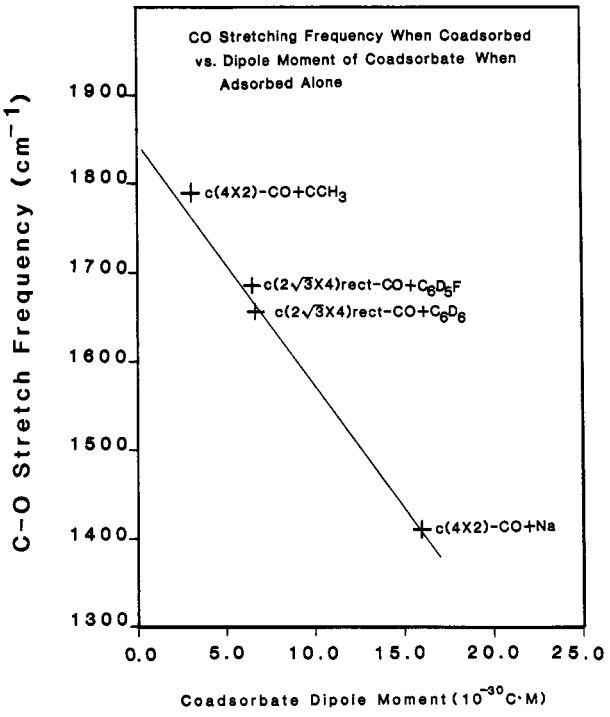


Figure 19
The C-O stretching frequency in structures that have one CO per coadsorbate is plotted against the effective surface dipole moment of the coadsorbate when adsorbed alone on the Rh(111) surface.

coadsorbate the lower the C-O stretching frequency of coadsorbed CO. The reduction of CO stretching frequency is thought to originate from several effects: a Stark effect for CO coadsorbed with ethylidyne, benzene, and fluorobenzene (the decrease in CO stretching frequency is proportional to the electric field experienced by CO oriented along its axis), charge transfer through the metal into the CO $2\pi^*$ orbital, and even possibly the formation of a chemical complex for CO coadsorbed with sodium.

In summary, we find that CO induced ordering occurs when CO is coadsorbed with adsorbates that have an oppositely oriented surface dipole moment. Model calculations indicate that the attractive dipole-dipole interaction energy is largely responsible for the formation of ordered structures containing oppositely oriented dipoles.

## FUTURE STUDIES

The surface science techniques that have become available during the past two decades are eminently useful in studies of the structure and bonding of organic molecules adsorbed on metal surfaces. As a result of these studies the nature of the surface chemical bond of organic molecules is elucidated. The two examples given here, ethylene and benzene, indicate the uniqueness of the surface chemical bond. The temperature dependent sequential decomposition, the similarity of the strongly adsorbed surface species to organometallic multi-nuclear complexes all indicate the richness and diversity of two dimensional organic chemistry. The available experimental results also indicate that the strongly adsorbed organometallic species on the surface play only secondary or peripheral roles in catalytic organic surface reactions. These reactions occur either on top of these strongly adsorbed organic species or on bare metal sites embedded into these organometallic two dimensional layers. It is imperative, that in the future, we study the organic surface chemistry of many molecules that are the derivatives of benzene as well as hetero nuclear organic molecules that contain nitrogen, sulfur or oxygen. Only after the accumulation of a great deal of data will the systematic patterns of the surface chemical bond emerge. Another direction that studies of organic monolayers will take is the investigations of their adsorption on surfaces with a large concentration of defects, steps and kinks. Up to now most of the studies of organic monolayers were focused on flat rather structurally uniform surfaces. The presence of defects have great catalytic significance. There are indications that bond breaking activities are very different at these differently coordinated surface sites. Another major area of organic surface chemistry for the future is the studies of organic molecules at solid-liquid and solid-solid interfaces.

The scanning tunneling microscope that has been discovered recently appears to be an excellent technique for a molecular level study of adsorbed organic monolayers at solid-liquid interfaces. Another technique that opens up investigations at solid-liquid interfaces is second harmonic generation. This technique uses the non-linear behavior of lasers to investigate the surfaces by looking at the reflected signal at $2\omega$ after a photon of frequency $\omega$ is incident on the surface. The second harmonic generation is the property of the surface because of symmetry reasons. As a result, it is eminently useful to obtain molecular information on a fraction of a surface monolayer. This has been demonstrated in several studies that were published recently. A modified version of second harmonic generation is sum frequency generation that can produce vibrational spectra of adsorbed molecules at the solid-liquid and solid-solid interfaces. This technique has great significance in studies of corrosion and lubrication. Studies of this sort could also be carried out in a diamond anvil to study organic monolayers between two solid surfaces. Diamond anvils can achieve high pressures that are rather important in surface science and occur under conditions of wear and lubrication. It is hoped that the bonding and orientation of organic molecules will be uncovered in this circumstance by diamond anvil studies using second harmonic generation for example. It is hoped that researchers in the field of surface science and organic chemistry will consider investigations in these frontier areas of surface organic chemistry.

## Acknowledgements

This work was supported by the Director, Office of Energy Research, Office of Basic Energy Sciences, Materials Sciences Division, U.S. Dpartment of Energy under Contract Number DE-AC03-76SF00098.

## REFERENCES

1. G.A. Somorjai, Chemistry in Two Dimensions; Cornell University Press: Ithaca, NY, 1981.

2. M.A. Van Hove, S.Y. Tong, Surface Crystallography by Low Energy Electron Diffraction: Theory, Computation and Structural Results; Springer: Heidelberg, 1979.

3. H. Ibach, D.L. Mills, Electron Energy Loss Spectroscopy and Surface Vibrations; Academic: New York, 1982.

4. D.F. Ogletree, J.E. Katz, G.A. Somorjai, Rev. Sci. Instrum. 57(12), 3012-3018(1986).

5. M.A. Van Hove, R.F. Lin, G.A. Somorjai, Phys. Rev. Lett. 51, 778(1983).

6. D.K. Saldin, J.B. Pendry, M.A. Van Hove, G.A. Somorjai, Phys. Rev. B B31, 1216(1985).

7. M.R. Albert, J.T. Yates, Jr., The Surface Scientist's Guide to Organometallic Chemistry; American Chemical Society: Washington, DC, 1987.

8. D.W. Blakely, E.I. Kozak, B.A. Sexton, G.A. Somorjai, J. Vac. Sci. Technol. 13, 1091(1976). A.L. Cabrera, N.D. Spencer, E.I. Kozak,P.W. Davies, G.A. Somorjai, Rev. Sci. Instrum. 53, 1888(1982).

9. M. Salmeron, G.A. Somorjai, J. Phys. Chem. 86, 341(1982).

10. H. Steininger, H. Ibach, S. Lehwald, Surf. Sci. 117, 685(1982).

11. B.E. Bent, Ph.D. Thesis, University of California, Berkeley, (1986).

12. R.J. Koestner, M.A. Van Hove, G.A. Somorjai, Surf. Sci. 121, 321(1982); J. Phys. Chem. 87, 203(1983).

13. N.R. Avery, N. Sheppard, Proc. R. Soc. London A 405, 1(1986). (a) J.E. Demuth, H. Ibach, Surf. Sci. 78, 1238(1978). A.M. Baro, H. Ibach, J. Chem. Phys. 74, 4194(1981). L.L. Kesmodel, G.D. Waddill, J. Gates, Surf. Sci. 138, 464(1984). J.A. Stroscio, S.R. Bare, W. Ho, Surf. Sci. 148, 499 (1984). M.M. Hills, J.E. Parmeter, C.B. Mullins, W.H. Weinberg, J. Am. Chem. Soc. 108, 3554(1986).

14. D.B. Kang, A.B. Anderson, Surf. Sci. 1985, 155, 639.

15. C.M. Mate, G.A. Somorjai, Surf. Sci. 160(1985) 542.

16. M.A. Van Hove, R.F. Lin, G.A. Somorjai, J. Am. Chem. Soc. 108 2532(1986).

17. M.A. Van Hove, R.F. Lin, D.F. Ogletree, G.S. Blackman, C.M. Mate, G.A. Somorjai, J. Vac. Sci. Technol. A5 692(1987).

18. D.F. Ogletree, M.A. Van Hove, G.A. Somorjai, Surf. Sci. 183 1(1987).

19. H. Ohtani, M.A. Van Hove, M.A. Somorjai, Surf. Sci. 187, 372(1987).

20. B.E. Bent, C.M. Mate, J.E. Crowell, B.E. Koel, G.A. Somorjai, J. Phys. Chem. 91, 493(1987).

21. M.P. Gomez-Sal, B.F.G. Johnson, T. Lewis, P.R. Raithby, A.H. Wright, J. Chem. Soc. Chem. Commun. 1682 (1985).

22. B.E. Koel, J.E. Crowell, B.E. Bent, C.M. Mate, G.A. Somorjai, J. Phys. Chem. 90, 2949(1986).

23. C.M. Mate, H.W.K. Tom, X.D. Zhu, Y.R. Shen, G.A. Somorjai, J. of Chem. Phys. 88, 441(1988).

24. C.M. Mate, B.E. Bent, G.A. Somorjai, J. Electron Spectrosc. Related Phenomena 39 (1986) 205.

25. C.M. Mate, C.-T. Kao, B.E. Bent and G.A. Somorjai, Surf. Sci. in press.

26. C.M. Mate, Ph.D. Thesis, University of California, Berkeley, 1986.

27. G.S. Blackman, C.-T. Kao, B.E. Bent, C.M. Mate, M.A. Van Hove and G.A. Somorjai, submitted to Surf. Sci. (1988).

28. B.E. Bent, C.-T. Kao, A. Slavin, G.A. Somorjai, J. Phys. Chem. in press.

29. H. Ohtani, C.-T. Kao, M.A. Van Hove, G.A. Somorjai, (book) Progress in Surf. Sci. 23, 155-316(1987).

30. R.F. Lin, G.S. Blackman, M.A. Van Hove, G.A. Somorjai, Acta Crystallographia B43 368(1987).

31. H. Ohtani, M.A. Van Hove, G.A. Somorjai, ICSOS Proceedings (1987) in press.

32. H. Ohtani, M.A. Van Hove, G.A. Somorjai, J. Phys. Chem. in press.

33. H. Ohtani, M.A. Van Hove, G.A. Somorjai, J. Phys. Chem. in press; H. Ohtani, B.E. Bent, C.M. Mate, M.A. Van Hove, G.A. Somorjai, Appl. Surf. Sci. in press.

34. R.A. dePaola, J. Hrbek, F.M. Hoffmann, J. Chem. Phys. 82, 2484(1985).

35. L.J. Whitman, W. Ho, J. Chem. Phys. 83, 4808(1985).

36. L. Westerlund, L. Jonsson, S. Andersson, Surf. Sci. 187, L669(1987).

37. R.J. Koestner, M.A. Van Hove, G.A. Somorjai, Surf. Sci. 107, 439(1981).

38. J.E. Crowell, G.A. Somorjai, Appl. Surf. Sci. 19, 73(1984).

39. J.R. MacDonald, C.A. Barlow, Jr., J. Chem. Phys. 39, 412(1963); J.R. MacDonald, C.A. Barlow, Jr., J. Chem. Phys. 44, 202(1966).

40. M.A. Van Hove, R.J. Koestner, G.A. Somorjai, Phys. Rev. Letters 50 903(1983).

41. J.E. Crowell, Ph.D. Thesis, University of California, Berkeley, 1984, unpublished.

42. J.K. Norskov, S. Holloway, N.D. Lang, J. Vac. Sci. Technol. A3 1668(1985); N.D. Lang, S. Holloway, J.K. Norskov, Surf. Sci. 150, 24(1985).

43. A. Gavezzotti, M. Simonetta, M.A. Van Hove, G.A. Somorjai, Surf. Sci. 154, 109(1985).

44. R. West, D. Eggerding, J. Perkins, D. Handy, E.C. Tuazon, J. Am. Chem. Soc. 101, 1710(1979).

45. E. Ruckenstein, T. Halachev, Surf. Sci. 122, 422(1982).

46. M.E. Dry, T. Shingles, L. J. Boshoff, G.J. Oosthuizen, J. Catal. 15 190(1969).

47. E.L. Garfunkel, J.E. Crowell, G.A. Somorjai, J. Phys. Chem. 86, 310(1982).

48. J. Lee, C.P. Hanrahan, J. Arias, R.M. Matin, H. Metiu, Phys. Rev. Letters 51, 1803(1983).